Babol Noshirvani University of Technology

Journal of Structural and Earthquake Engineering

Research Paper

Numerical Investigation of the Effect of Boundary Conditions on the Out-of-Plane Seismic Performance of Masonry Infill Walls

Delaram Ostad [1], Jalil Shafaei [2], Farnoosh Basaligheh[3], Mohammad Javad Zarei[4], Mohammad Javad Esmaeili[4], Milad Faraji[4], AmirAli Fakor Yekta[5]

[1] PhD student, Department of Civil Engineering, Shahrood University of Technology, Shahrood, Iran, E-mail address: Delaramostad@shahroodut.ac.ir
[2] Associate Professor, Department of Civil Engineering, Shahrood University of Technology, Shahrood, Iran, E-mail address: js.shafaei@gmail.com
[3] Assistant Professor, Department of Civil Engineering, Shahrood University of Technology, Shahrood, Iran, E-mail address: f_basaligheh@yahoo.com
[4] M. Sc. student, Department of Civil Engineering, Shahrood University of Technology, Shahrood, Iran,
[5] Undergraduate student, Department of Civil Engineering, Shahrood University of Technology, Shahrood, Iran,

Article information

Received: March 15 2025.

Revised: April 30 2025.

Accepted for publication: May 25 2025.

Corresponding author:

J.Shafaei(jshafaei@shahroodut.ac.ir).

Abstract

Out-of-plane failure of masonry infill walls is a critical issue affecting the seismic performance of reinforced concrete (RC) frame structures, especially during strong ground motions. While infill walls enhance the in-plane stiffness of RC frames, they remain highly vulnerable to out-of-plane actions perpendicular to their surface. This study presents a detailed numerical investigation of the out-of-plane behaviour of masonry infill walls with various boundary conditions using the finite element software ABAQUS. Four support configurations were considered: infills supported on four sides, three sides, two horizontal sides, and one side. The analyses focused on deformation patterns, stress distribution, and failure mechanisms under out-of-plane loading. The results demonstrate that boundary conditions have a significant influence on wall stiffness, strengt h, and overall stability. Full boundary confinement (four-sided support) markedly improves performance through the development of a two-way arching mechanism. Quantitatively, the four-sided infills exhibited approximately 73% higher out-of-plane strength than the three-sided configuration, about 34% higher than the two-sided configuration, and substantiall y greater resistance than the single-sided case. These findings highlight the crucial role of boundary support in the seismic ev aluation and retrofitting of infilled RC frame structures.

Keywords: Masonry infill; Out-of-plane loading; Boundary conditions; Seismic performance; ABAQUS; Failure mechanis m.

1. Introduction

Masonry infill walls are commonly used in reinforced concrete (RC) frame structures for both architectural and functional purposes. Although traditionally regarded as non-structural components, their presence significantly affects the overall seismic behaviour of RC frames. One of the key vulnerabilities observed in past earthquakes is the out-of-plane failure of infill walls, which can lead to hazardous debris, loss of enclosure, and even progressive collapse of adjacent structural elements.

Out-of-plane failure occurs when seismic forces acting perpendicular to the wall surface exceed the limited flexural or arching capacity of the infill, particularly when the wall is inadequately connected to the surrounding frame. This failure mechanism becomes more critical when boundary support is reduced due to poor construction practices, material degradation, or prior in-plane damage. Field observations from major earthquakes, such as those in Nepal (2015), Kermanshah (2017), and Spain (2011), have demonstrated the severity and frequency of this type of failure (Fig. 1).

(a) (b) (c)

Fig. 1. Out-of-plane collapse of masonry infill walls observed during past earthquakes ;(a) Nepal earthquake, 2015 [1]; (b) Kermanshah earthquake, 2017 [2]; (c) Spain earthquake, 2011 [3].

While numerous studies have investigated the in-plane behaviour of infill walls, relatively few have focused exclusively on their out-of-plane performance. Those that have done so often examine the influence of boundary conditions, support configurations, and wall geometry, as these parameters substantially affect load transfer mechanisms, failure modes, and energy dissipation capacity. However, experimental studies on out-of-plane behaviour under seismic conditions remain challenging due to the complexity of replicating realistic dynamic loads and boundary constraints.

Several experimental and numerical investigations have been conducted to evaluate the out-of-plane performance of masonry infills. Early studies by Dawe and Seah [8] and Negro and Verzeletti [9] demonstrated the significant role of boundary conditions in determining the strength and failure mechanisms of infill walls under lateral loads. Subsequent works by Daphnis et al. [10] and Ando et al. [11], based on full-scale experimental testing, further emphasized the importance of edge restraint. More recent research by Liu et al. [12], Rabinovich and Madah [13], and Furtado et al. [1,14] utilized finite element modeling to explore various infill configurations and assess their seismic resistance. Additionally, Wang [15] and Hashemi and Mosalam [4] investigated the dynamic response of infill walls using advanced numerical modeling and shake-table experiments, highlighting the need to consider the interaction between in-plane and out-of-plane behaviours in performance-based seismic design.

Noh et al. [16] and Di Domenico et al. [17] further analyzed the effects of geometric variations and partial boundary conditions on out-of-plane response. Regarding interaction effects, the studies by Angel and Abrams [5], Tasnimi and Zamordian [6], and Kumarani et al. [7] illustrated the complexities associated with bi-directional loading. Nevertheless, as Messali et al. [18] concluded, the literature still lacks consensus on the significance and modeling of these interactions.

In this context, finite element (FE) modeling provides an effective means of investigating the out-of-plane behaviour of infill walls under controlled yet realistic loading conditions. The present study employs the finite element software ABAQUS to model the nonlinear out-of-plane response of masonry infill walls with different boundary conditions. Four configurations are analyzed: walls supported on four sides, three sides, two horizontal sides, and one side only. Through nonlinear static (pushover) analyses, the study evaluates the influence of boundary support on the stiffness, strength, and failure mechanisms of infill walls subjected to out-of-plane seismic loading.

The results of this research provide valuable insight into the role of boundary conditions in governing the out-of-plane vulnerability of infill walls and offer guidance for developing improved seismic design and retrofitting strategies. The novelty of this study lies in the systematic numerical assessment of varying boundary conditions, which clarifies their influence on stiffness degradation, strength reduction, and failure modes. The outcomes contribute to a more comprehensive understanding of the out-of-plane seismic behaviour of infilled RC frames and support the advancement of performance-based retrofit approaches for existing structures.

2. Models for Predicting the Out-of-Plane Capacity of Masonry Infill Walls

The out-of-plane behaviour of masonry infill walls can generally be classified according to two primary resisting mechanisms: flexural action and arching action. Accurate representation of these mechanisms is essential for evaluating the out-of-plane seismic capacity of infill panels in reinforced concrete (RC) frame structures.

2.1. Flexural Action-Based Models

Flexural action-based models assume that the infill wall behaves as a vertical plate subjected to a uniform lateral pressure. The out-of-plane capacity in this case is mainly governed by the flexural strength of the masonry, defined as the maximum uniform pressure that causes collapse. Early analytical models derived from Timoshenko's classical plate theory [19–22] assumed linear-elastic bending behaviour. However, these models fail to capture the highly nonlinear response of masonry under actual loading conditions.

To overcome these limitations, researchers such as Heseltine and Hendry introduced modified formulations that incorporate nonlinear effects through yield-line theory and the orthogonal tensile strength of masonry [22]. These approaches estimate the out-of-plane resistance by evaluating the effective moment capacity along critical failure planes, typically aligned with the mortar bed joints. Despite their simplicity and theoretical clarity, flexural-based models tend to underestimate the actual out-of-plane strength, as they neglect the contribution of compressive forces that develop through arching action once cracking occurs.

2.2. Arching Action-Based Models

When masonry infills crack due to lateral displacement or seismic demand, they often develop an alternate load-resisting mechanism: arching action. In this mode, the cracked infill redistributes compressive stresses toward its supported boundaries, generating a load path through compressive struts. Experimental and analytical observations confirm that arching can significantly enhance the out-of-plane resistance beyond that predicted by flexural models alone [23].

After the initial cracking, the infill behaves like a three-pin arch (Fig. 2b), where the wall segments rotate as rigid bodies around their supports, forming a compressive zone at mid-height. Two dominant failure mechanisms can occur under arching: (1) crushing of the masonry at the compressed regions, and (2) detachment or gap formation between the infill and surrounding frame. These mechanisms are directly influenced by the boundary conditions, such as the number of supported edges, frame stiffness, and mortar joint characteristics.

Overall, arching action provides a more realistic and generally conservative estimate of the out-of-plane strength for masonry infills, particularly when they are laterally confined on three or four edges. Numerical simulations using finite element models, such as those developed in ABAQUS, allow for detailed analysis of both flexural and arching behaviour under varying boundary conditions.

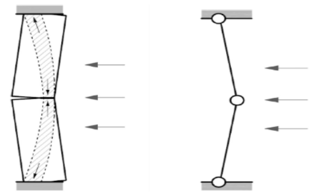

Fig. 2. Arching mechanism of masonry infill walls: (a) physical representation; (b) idealized three-hinged arch mechanism [23].

2.3. Effect of Boundary Conditions on Arching Action in Out-of-Plane Loading

The boundary conditions of masonry infill walls significantly influence their ability to develop arching action under out-of-plane loading. Unlike ductility-based failures, arching action provides a mechanism for resisting lateral pressure through compression rather than flexure, leading to increased strength in appropriately confined infills.

The significance of arching action was first highlighted by McDowell et al. (1956), who observed that unreinforced masonry (URM) walls in laboratory tests displayed out-of-plane capacities up to six times higher than those predicted by simple slab theory. McDowell attributed this enhanced resistance to the development of compressive forces resulting from arching action, a hypothesis that has since become a fundamental concept in masonry wall behaviour under seismic loading [24]. Three typical boundary conditions govern the type and effectiveness of arching action:

Fully supported infill (four edges bounded): When the infill is restrained on all four sides by the surrounding frame (i.e., columns and beams), a two-way arching mechanism develops. In this case, compressive stresses are distributed both vertically and horizontally, significantly enhancing the wall's out-of-plane capacity (Fig. 3a).

Three-edge support (e.g., beam gap or column gap): If one side of the infill is unrestrained, typically at the top or sides, only one-way arching action occurs. This condition limits the compressive stress path to a single direction, reducing the effectiveness of arching (Fig. 3b, 3c).

Two-edge support (double-gapped infill): When the infill is bounded only on two parallel edges (e.g., top-bottom or left-right), a pure one-way arching mechanism is formed. This case represents the weakest boundary configuration with minimal confinement and lowest out-of-plane resistance, as load redistribution is limited to a single arching axis (Fig. 3c).

The degree of edge restraint not only influences the strength and stiffness of the infill but also its failure mode, (Fig. 4 and Fig. 5). Fully confined infills tend to fail by crushing at compressive regions, whereas partially supported ones are prone to detachment or overturning. Therefore, understanding the relationship between boundary conditions and arching action is critical for evaluating the seismic vulnerability of masonry-infilled RC frames.

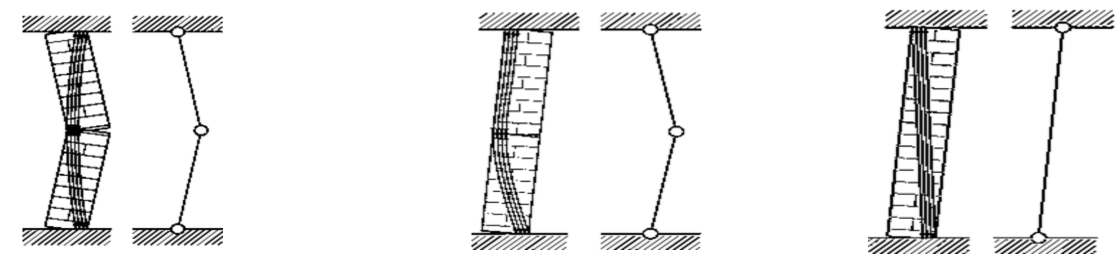

(a) three-hinged arching action; (b) three-hinged gapped arching action; (c) two-hinged arching action;

Fig. 3. Side-view profiles of vertical strips under different boundary conditions [25].

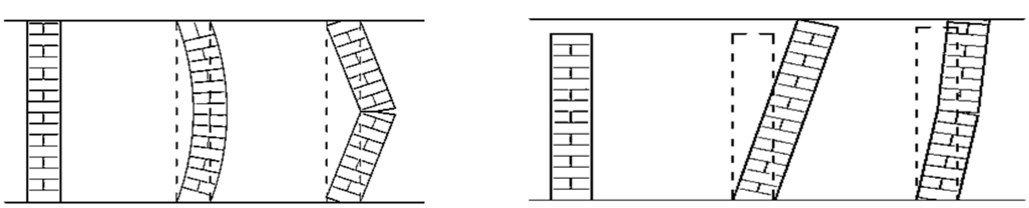

(a) Rigid arching action development; (b) Gapped arching action development;

Fig. 4. Development phases of arching action under different boundary conditions [25].

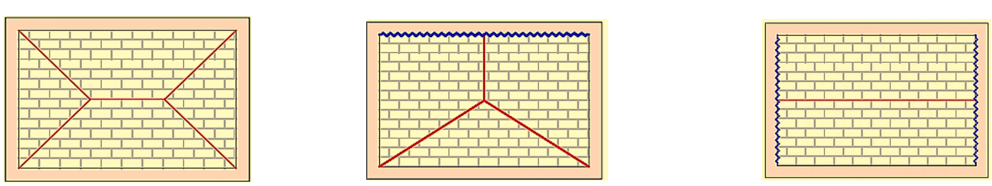

a. Two-way (rigid) arching action
b. Gapped arching action
c. One-way (double-gapped) action

Fig. 5. Types of arching action in masonry infill walls under different boundary conditions [25].

3. Numerical Modeling

In this study, numerical models were developed to investigate the out-of-plane behaviour of masonry infill walls with various boundary conditions. The modeling was based on the experimental configuration of Mansouri et al. (2014) [26], who tested half-scale (1:2) masonry-infilled reinforced concrete (RC) frames. The frame system consisted of a single-bay, single-story RC structure, infilled with solid clay masonry units.

3.1. Geometrical Configuration of Models

The masonry panel dimensions were 2100 mm in length, 1300 mm in height, and 106 mm in thickness, while the clay bricks used in the infill measured 310 mm (length) × 490 mm (height) × 106 mm (thickness). The brick arrangement followed a regular bonding pattern representative of typical construction practices in the region (Fig. 7). The geometry of the RC frame and infill wall is shown in Fig. 6.

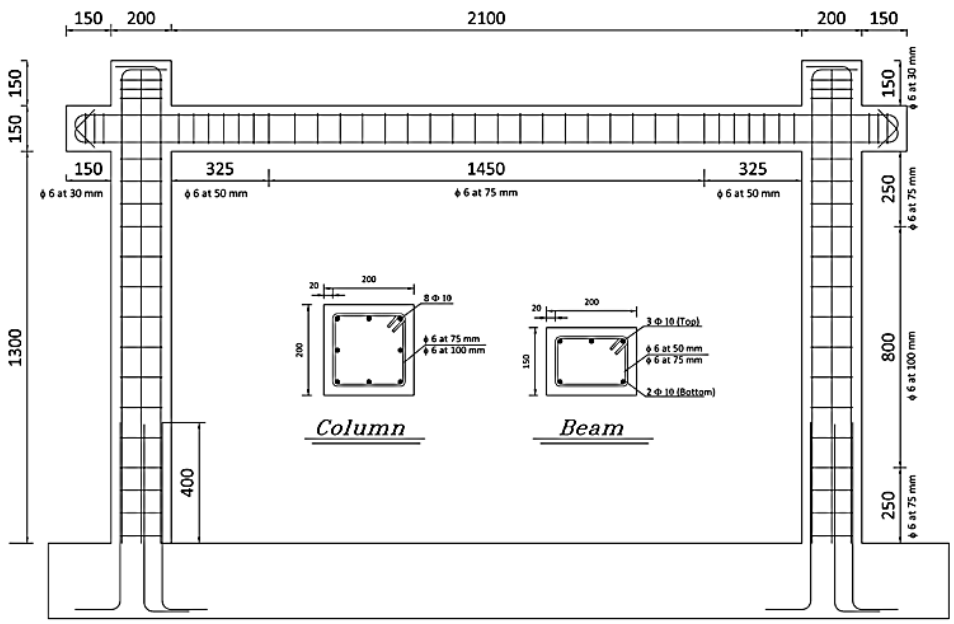

Fig. 6. Geometry and reinforcement details of the reinforced concrete frame and infilled masonry wall (dimensions in millimeters) [26].

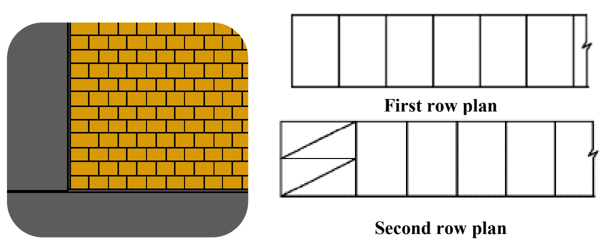

Fig. 7. Brick arrangement in the infilled masonry wall.

3.2. Boundary Condition Scenarios

To evaluate the influence of boundary conditions on the out-of-plane response, four distinct support configurations between the RC frame and the masonry infill were modeled, as shown in Figure 8. These conditions simulate realistic construction scenarios and allow the identification of dominant failure mechanisms (i.e., flexural versus arching action) under out-of-plane seismic demands.

Fully Bounded Infill (Four-Sided Support) – The infill was in full contact with the surrounding RC frame on all four edges, allowing for the development of two-way arching action and providing the highest expected out-of-plane resistance (Fig. 8a).

Three-Sided Support – The infill was detached from the top beam by the thickness of one brick, simulating a discontinuity at the top edge. This setup restricts arching action primarily to one direction and weakens confinement (Fig. 8b).

Two-Sided Horizontal Support – The infill was detached from both columns, with vertical gaps equivalent to one brick thickness, while the top and bottom remained in contact. This configuration permits limited one-way arching action in the vertical direction (Fig. 8c).

One-Sided Support – The infill was separated from the top beam and both side columns, maintaining contact only at the bottom. This case represents the most vulnerable configuration, where arching action is nearly absent, and the infill behaves more like an unsupported panel under lateral loading (Fig. 8d).

These varying boundary conditions were incorporated into finite element models using ABAQUS software. The purpose was to simulate and compare the out-of-plane displacement capacity and failure mechanisms across all configurations. Nonlinear static analyses (pushover) were performed, enabling an in-depth evaluation of the influence of edge support on out-of-plane seismic performance.

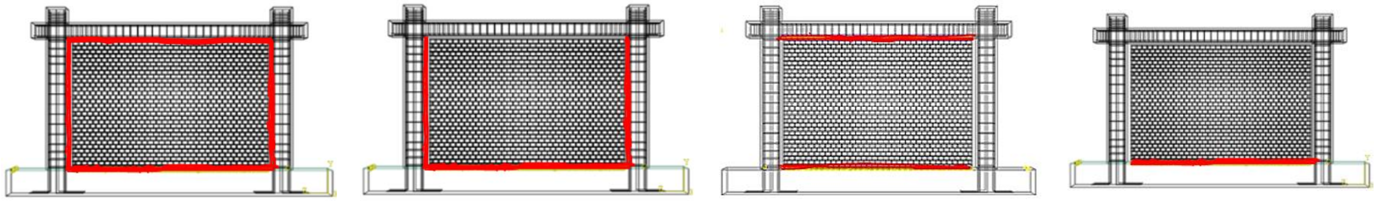

a. Connect on 4sides b. Connect on 3sides c. Connect on 2sides d. Connect on 1sides

Fig. 8. Connection details between infilled masonry and the reinforced concrete frame.

3.3. Material Properties

The material properties used in the numerical simulations were directly adopted from the experimental study by Mansouri et al. (2014) [26], who conducted comprehensive tests on masonry, concrete, and reinforcing steel. Their reported results include compressive strengths of concrete, solid bricks, and masonry prisms, as well as shear strength of mortar, in accordance with ASTM standards, Table 1. These experimentally derived values were used as input parameters in ABAQUS to model the out-of-plane response of masonry infills under various boundary conditions.

Table 1. Test results of materials (MPa) [26]

Material	Property	Value
Concrete	Compressive Strength	21.9
Brick Units	Compressive Strength	9.16
Mortar	Compressive Strength	8.33
Masonry	Compressive Strength	2.3
	Elastic Modulus	437
	Mortar Joint Shear Strength	0.31
Longitudinal Steel Reinforcements	Yield Strength	438.3
	Ultimate Strength	645
Transverse Steel Reinforcements	Yield Strength	396.3
	Ultimate Strength	509.3

3.4. Out-of-Plane Load Calculation

The out-of-plane force applied to the masonry infill is calculated as the unit weight of the wall surface using the following equation:

$$w = \rho g * t$$
$$w = 185 \times 10^{-7} \left({}^{N}/_{mm^3}\right) * 106\ (mm) = 0.00196 \cong 0.002g\ \left({}^{N}/_{mm^2}\right) \quad (1)$$

Accordingly, the out-of-plane surface load for different acceleration levels is obtained by multiplying this base value by the acceleration factor. The resulting loads are summarized in the Table 2:

Table 2. Out-of-plane load at different acceleration levels (N/mm^2).

Loading at different acceleration levels	Value of out-of-plane load on the surface
1g	0.002
2g	0.004
4g	0.008
6g	0.012
8g	0.016
10g	0.02

4. Discrete Finite Element Model

The numerical simulations were carried out in ABAQUS using a meso-scale finite element modeling approach to investigate the out-of-plane behaviour of reinforced concrete (RC) frames with masonry infills. Concrete, brick units, and mortar were modeled using C3D8R solid elements, while steel reinforcements were represented by T3D2 truss elements embedded within the concrete matrix. A mesh sensitivity analysis was performed using three mesh sizes: 100 mm for the coarse mesh, 50 mm for the medium mesh, and 25 mm for the fine mesh, to determine the optimal element discretization. The results revealed that the difference in peak load between the medium and fine meshes was less than 3%, while the coarse mesh led to a noticeable reduction in stiffness. Therefore, an element size in the range of 25 to 50 mm was adopted as an optimal compromise between numerical accuracy and computational efficiency. This modeling strategy ensured a reliable representation of material interactions, stress transfer mechanisms, and damage evolution under different boundary conditions.

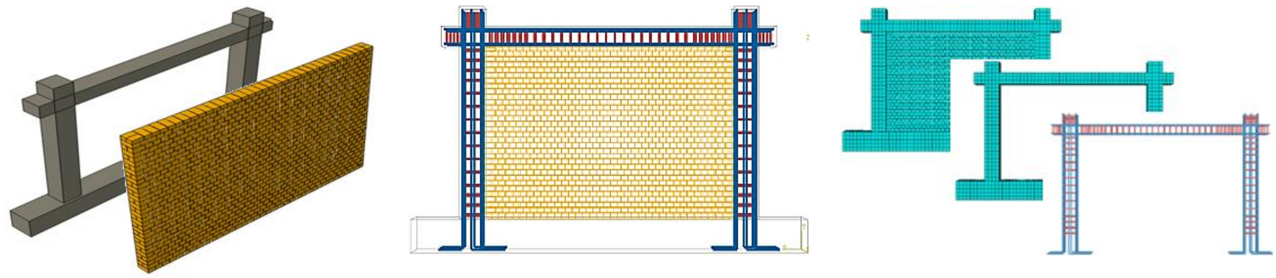

Fig. 9. Mesh and schematic representation of the reinforced concrete frame and masonry infill.

4.1. Surface-Based Cohesive Behaviour

To simulate the interaction and failure mechanisms between masonry units and mortar, surface-based cohesive behaviour with traction-separation laws was employed in ABAQUS. This approach includes linear elastic behaviour, damage initiation, and damage evolution. Uncoupled traction-separation behaviour was assumed, and cohesive stiffness was defined based on elastic properties of materials. Normal contact was modeled as hard contact, and tangential behaviour included friction-based sliding. Shear failure occurs when interfacial stress exceeds mortar shear strength. The mechanical properties of masonry bricks and interface parameters used in the model are listed in Tables 3 and 4.

Table 3. Mechanical specification of interface contact.

Reference Specimens	Tension		Shear			Joint			
	G_f^I $(N.mm/mm^2)$	f_t (N/mm^2)	G_f^{II} $(N.mm/mm^2)$	$C = 1.4f_t$ (N/mm^2)	$\mu = tan\theta$	k_{nn} (N/mm^3)	k_{ss} (N/mm^3)	k_{tt} (N/mm^3)	
SOLID	0.012	0.24	0.05	0.16	0.75	110	50	50	Hard

Table 4. Mechanical parameters used in the Concrete Damaged Plasticity model for the analytical specimens.

Bare Frame	Material	Dilation Angle	Eccentricity	σ_{bo}/σ_{co}	k	Viscosity Parameter
Bare Frame	concrete	30	0.1	1.16	0.667	0.001
Infilled frame	concrete	30	0.1	1.16	0.667	0.001
	Unit Brick	10	0.1	1.16	0.67	0.001

4.2. Analysis Methods

To reduce convergence issues in nonlinear simulations of masonry-infilled RC frames, the explicit dynamic analysis method in ABAQUS was adopted. This approach, unlike the implicit method, avoids iterative procedures by using a central difference integration scheme. The analysis was performed quasi-statically in both in-plane and out-of-plane directions, using small time increments to ensure numerical stability.

4.3. Plastic Behaviour of the Brick Elements

The nonlinear behaviour of the brick units was modeled using the Concrete Damaged Plasticity (CDP) model in ABAQUS. Although originally developed for concrete, this model is widely applicable to other brittle materials such as masonry bricks. It accounts for two primary failure mechanisms: tensile cracking and compressive crushing. The evolution of the yield surface is governed by two hardening variables related to tensile and compressive plastic strains. Moreover, CDP captures the stiffness degradation under cyclic loading, as illustrated in Fig. 10, making it suitable for simulating the damage accumulation in masonry subjected to repeated or reversed loading.

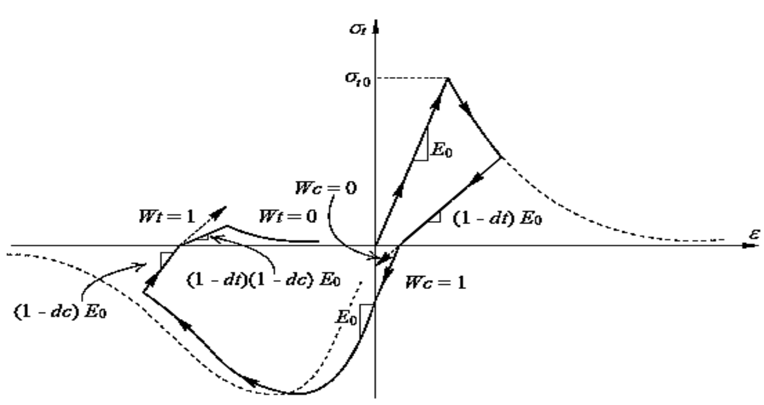

Fig. 10. Concrete behaviour in uniaxial loading [27].

4.4. Bilinear Method

To determine the ductility capacity of the infilled frame specimens, where the load–displacement curves lack a clear yield point, the idealized bilinear approach proposed by Pauli and Priestley was applied. As illustrated in Fig. 11, the bilinear envelope is constructed by identifying the yield displacement (δ_y) as the intersection of a secant line from the origin to the point corresponding to either the first yielding of longitudinal reinforcement or 75% of the ultimate load (P_U), whichever occurs earlier. The ultimate displacement (δ_u) is taken as the displacement at which the load falls to 80% of P_U. Using this method, the effective stiffness (K_e) and ductility (μ) are calculated based on Equations (2) and (3):

$$K_e = \frac{P_U}{\delta_y} \tag{2}$$

$$\mu = \frac{\delta_u}{\delta_y} \tag{3}$$

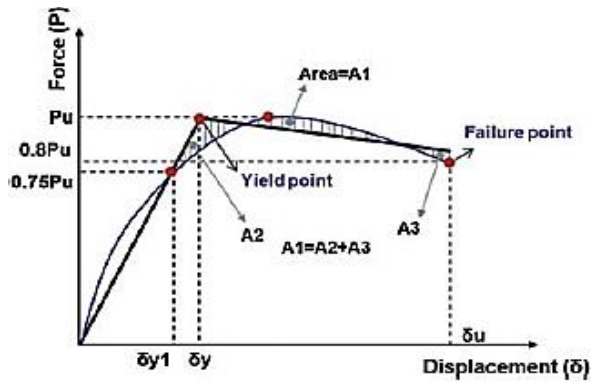

Fig. 11. Bilinearization using priestly & Pauli method [28].

5. Validation Models

The numerical modeling approach adopted in this study was primarily validated using the experimental specimens of Mansouri et al. [26], ensuring that the RC frame and masonry infill were accurately simulated before further analyses. The validation results of Mansouri's specimens are presented in Fig. 12 and Table 5, confirming the model's capability to capture in-plane behaviour through comparisons of strength, stiffness, ductility, and failure modes, Fig. 13 and Fig. 14. For out-of-plane behaviour, since Mansouri's study lacked out-of-plane testing, experimental data from Furtado et al. [29] were used. The numerical model was able to reproduce key damage patterns, including diagonal and vertical cracking indicative of two-way arching action. The force-displacement response and failure mode of the Furtado specimen, shown in Fig. 15 and Fig.16 and Table 6, demonstrate a strong correlation with the numerical predictions. These comparisons validate the model's effectiveness in capturing both in-plane and out-of-plane responses of masonry infilled frames.

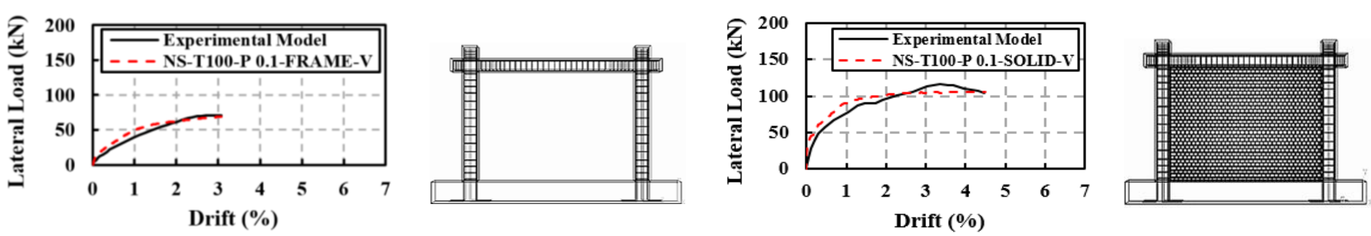

a. Frame b. Solid

Fig. 12. Verification of reference specimens.

Table 5. Comparison of experimental reference specimen and analytical specimen.

Specimens	Type Specimens	Lateral Load (kN)	Percentage difference	Effective Stiffness (kN/mm)	Percentage difference	Ductility	Percentage difference	Area below the chart (mm)	Percentage difference
FRAME	Experimental	70	4.5%	2.6	21.4%	1.65	16.27%	1929	7.3%
	Analytical	67		3.7		2.6		2067	
SOLID	Experimental	115	7.14%	7.2	6%	4.16	6.97%	5341.8	2.9%

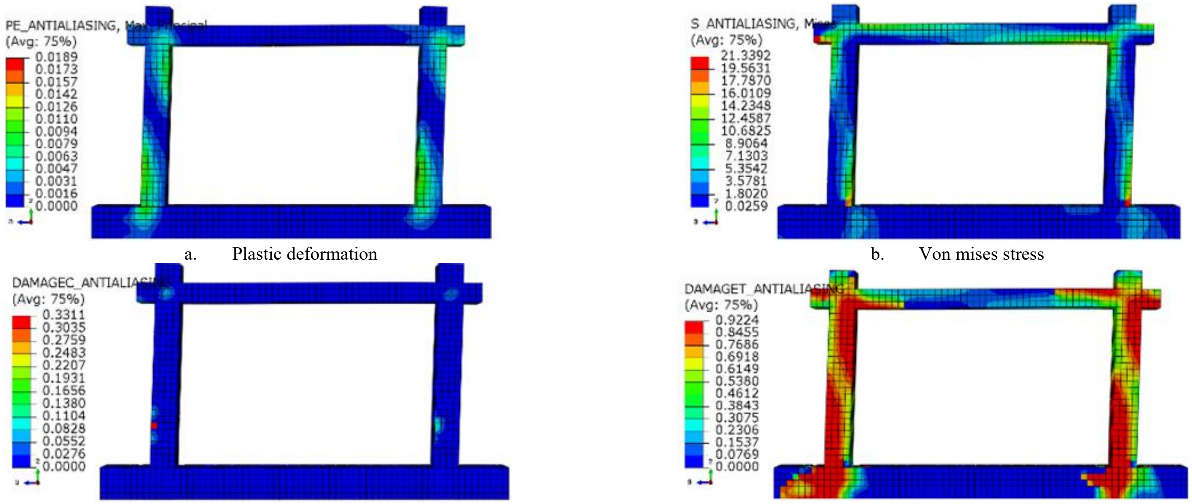

a. Plastic deformation b. Von mises stress

c. Compressive failure d. Tensile failure

Fig. 13. Damage and deformations of the non-seismic reinforced concrete frame specimen at 6% drift.

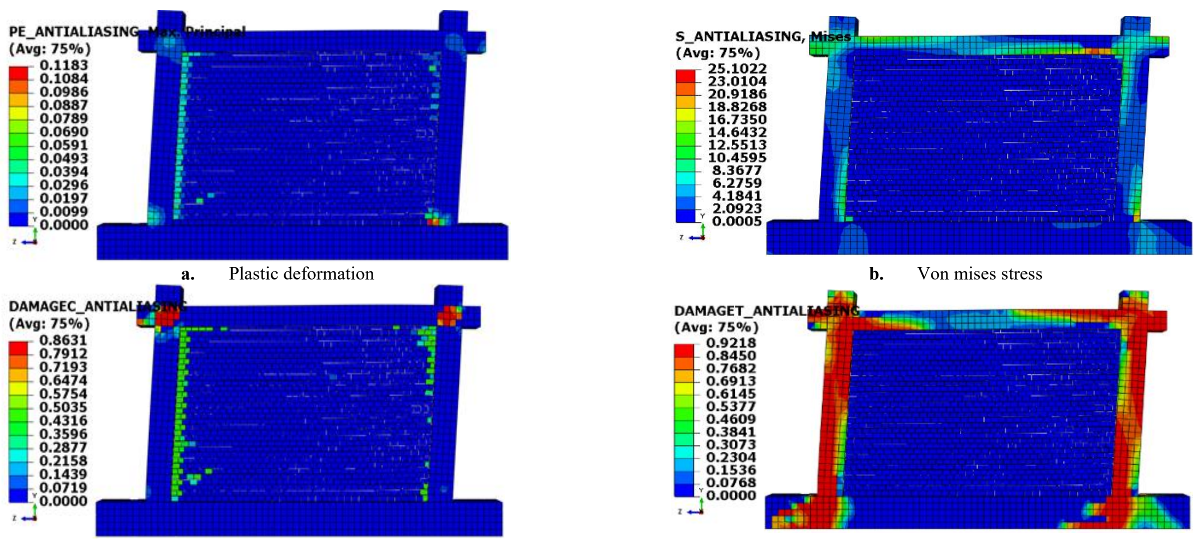

a. Plastic deformation **b.** Von mises stress

c. Compressive failure **d.** Tensile failure

Fig. 14. Damage and deformations of the masonry infilled frame specimen at 6% drift.

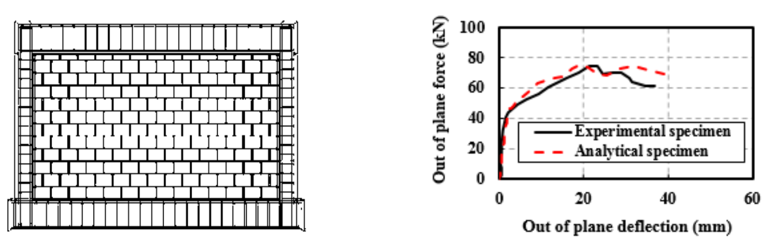

a. b.

Fig. 15. Verification of the non-seismic masonry infill-frame specimen under out-of-plane loading at 0.85% drift.

Table 6. Comparison of experimental reference and analytical specimen of Furtado et al.

Type Specimens	Lateral Load (kN)	Effective Stiffness (kN/mm)	Ductility	Area below the chart (mm)	Percentage difference (%)
Experimental	75	6.45	3.55	2281.44	11.9
Analytical	75.4	6.85	3.71	2554.5	

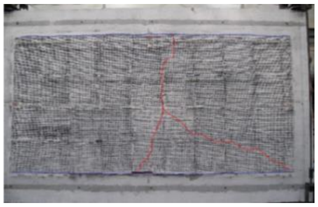

a. Experimental failure

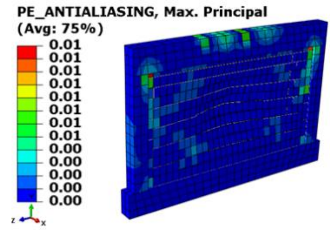

b. Plastic deformation

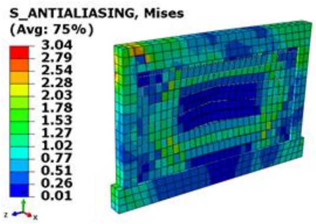

c. Von mises stress

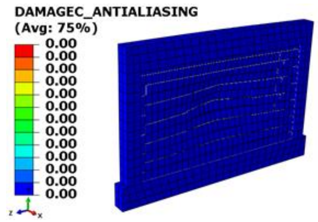

d. Compressive failure

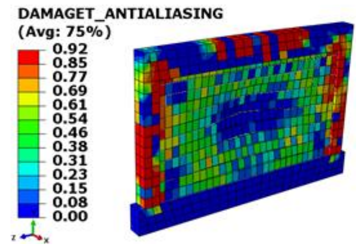

e. Tensile failure

Fig. 16. Damage and deformations of the reinforced concrete frame specimen under out-of-plane loading.

6. Results and Discussion

6.1. Out-of-Plane Behaviour

To investigate the effect of boundary conditions on the out-of-plane behaviour of masonry infill walls, four different connection configurations between the masonry and the surrounding RC frame were modeled in ABAQUS. The infills were subjected to gradually increasing acceleration levels, simulating lateral inertial loading from 1g to 10g, and their force–displacement behaviour was recorded.

As shown in Fig. 17, the specimens with more boundary constraints exhibited significantly higher out-of-plane strength and stiffness. The first specimen, with full four-side connection, exhibited the highest out-of-plane strength and smallest lateral displacement. This configuration benefited from a two-way arching action, which effectively distributed lateral loads and enhanced the load-carrying capacity, especially under higher acceleration levels up to 10g.

The second specimen, connected on three sides (with the top edge free), demonstrated a moderate performance. Its strength increased up to 3g, after which it began to degrade, and complete failure occurred around 6g. The lack of top restraint appears to significantly compromise the infill's ability to resist lateral forces, as it prevents the development of full arching action and introduces stress concentrations near the free edge.

The third configuration, where the top and bottom edges were connected but the vertical sides were free, showed higher resistance compared to the three-side connection. This specimen performed better under high accelerations (up to 10g) and displayed more ductile behaviour. The results suggest that horizontal support at top and bottom edges is more critical for out-of-plane performance than vertical edge support, likely because it allows better load redistribution and stability under vertical loading and rocking behaviour.

The fourth and weakest configuration involved connection on only one side (bottom edge). This specimen experienced immediate failure under the lowest applied acceleration (1g), indicating the inability of minimal boundary support to resist out-of-plane loading. The force–displacement curve in Fig. 17d confirms negligible strength and stiffness, and early collapse.

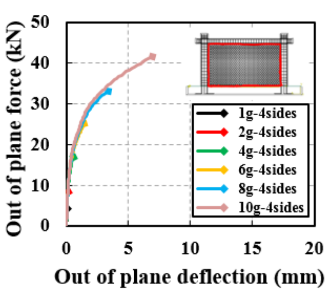

a. Connect on 4sides

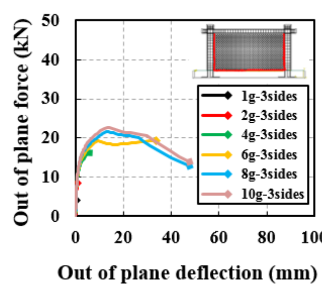

b. Connect on 3sides

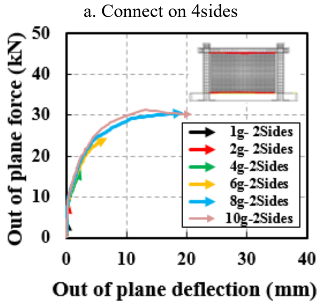

c. Connect on 2sides

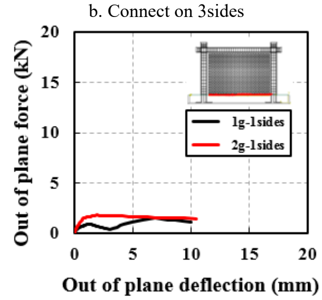

d. Connect on 1sides

Fig. 17. Out-of-plane loading at acceleration level and connect different.

6.2. Comparison of Specimen Responses

A comparative overview of all specimens is provided in Fig. 18, which clearly illustrates that increased connection surfaces enhance the infill's out-of-plane load resistance, stiffness, and energy absorption capacity. The effective stiffness and ductility were significantly higher in the four-side and two-horizontal-side connection configurations compared to others.

Interestingly, the stiffness remained relatively constant in the initial loading stages (1g–4g), particularly in better-confined specimens. This implies that initial deformations are minor, and the arching action remains largely intact. As acceleration levels increased (beyond 6g), notable reductions in stiffness were observed, particularly in less confined specimens, due to progressive cracking and loss of lateral load-carrying mechanism.

In conclusion, the simulation results underline the critical role of boundary conditions in out-of-plane performance of masonry infills. Full four-side confinement provides the best performance under inertial loading, followed by horizontal confinement. Reducing the number of connected edges leads to significant reductions in strength, stiffness, and stability. These insights are essential for seismic vulnerability assessment and retrofitting strategies of infilled RC frames.

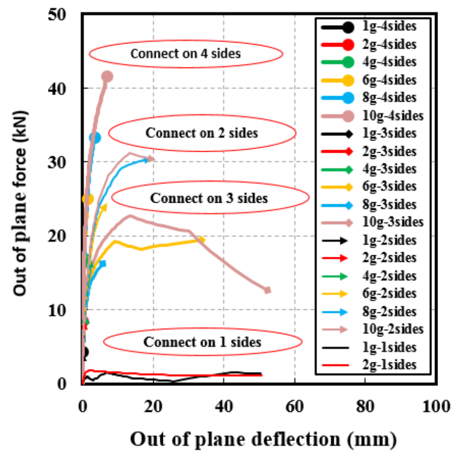

Fig. 18. Comparison of force–displacement curves under out-of-plane loading for infilled masonry walls with different connection details to the RC frame.

6.3. Bilinear Results and Plastic Deformation Patterns

Table 7 and Fig. 19 present a detailed comparison of the out-of-plane response of masonry infilled RC frames with different boundary conditions, focusing on lateral strength, effective stiffness, and plastic deformation patterns. The results indicate that the extent and configuration of boundary connections have a decisive influence on the structural behaviour under out-of-plane seismic loads.

The specimen with four-sided connections exhibited the best performance, achieving a maximum lateral load capacity of 41.6 kN and the highest effective stiffness of 11 kN/mm. The plastic deformation distribution shown in Fig. 19a is relatively uniform, particularly near the corners, reflecting a two-way arching mechanism and effective lateral load transfer.

In contrast, the three-sided connection with the top edge free reached a maximum lateral load of 24 kN, corresponding to a 42.3% reduction in strength compared to the fully supported case. Its stiffness also decreased to 4.3 kN/mm. As illustrated in Fig. 19b, stress concentrations and early cracking occurred along the unsupported top edge, indicating a loss of arching integrity and localized detachment.

The two horizontal side connection with top and bottom supported achieved a lateral strength of 31 kN and an effective stiffness of 8 kN/mm, performing better than the three-sided configuration. This represents a 25.5% reduction in strength relative to the four-sided specimen, yet it remains substantially stronger than the three-sided case. Fig. 19c shows a pronounced diagonal failure mode; however, the deformation is more stable due to the top and bottom confinement. This suggests that horizontal edge restraint reduces localized stress concentrations, thereby enhancing both lateral strength and deformation stability. In this configuration, the out-of-plane load is primarily resisted through flexural action between the supported edges rather than full two-way arching.

Finally, the one-sided connection exhibited the weakest performance, sustaining only 2 kN of lateral force, a 95% reduction relative to the four-sided configuration, with negligible stiffness of 1 kN/mm. Fig. 19d shows immediate detachment and toppling of the infill, highlighting the critical instability caused by minimal edge support.

Table 7. Bilinear analysis results for analytical specimens with connect different.

Type of connect frame with infill	Type loading (N/mm^2)	Lateral Load (kN)	Effective Stiffness (kN/mm)
Connect on 4sides specimens	Out of plane (10g)	41.6	11
Connect on 3sides specimens	Out of plane (10g)	24	4.3
Connect on 2sides specimens	Out of plane (10g)	31	8
Connect on 1sides specimens	Out of plane (10g)	2	1

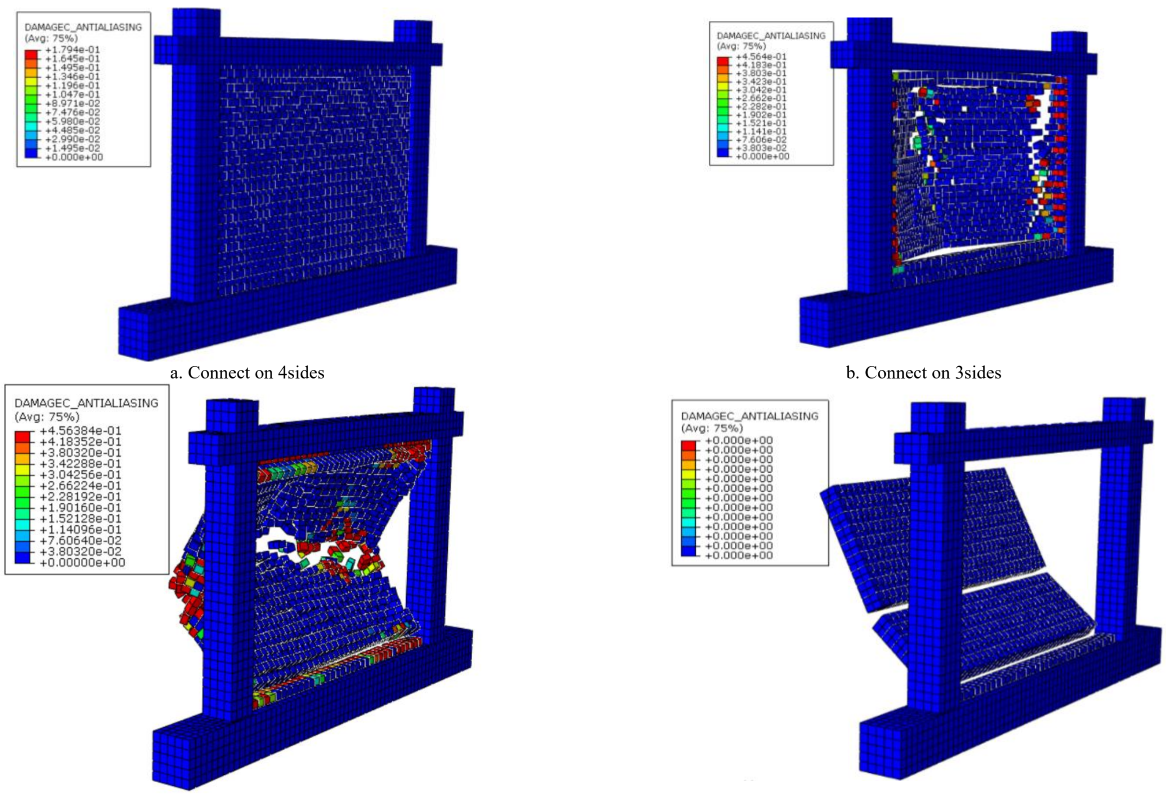

a. Connect on 4sides b. Connect on 3sides

c. Connect on 2sides d. Connect on 1sides

Fig. 19. Plastic deformations of various frame joints with masonry infill under out-of-plane loading.

The comparison between the two configurations revealed that the load transfer mechanism significantly depends on the direction and continuity of edge restraints. In the three-edge model with a free top, the absence of upper confinement limited the formation of a complete arch, causing stress concentration and premature cracking near the top corners. Conversely, the model with two horizontal supports (top and bottom) exhibited a vertical arching behaviour, where compressive forces were effectively distributed between the horizontal boundaries. This configuration demonstrated higher out-of-plane strength, stiffness, and overall stability

7. Conclusions

This study numerically investigated the out-of-plane behaviour of masonry infill walls under different boundary connection scenarios using ABAQUS. Four configurations were analyzed: infills supported on four sides, three sides (top free), two horizontal sides (top and bottom), and one side (bottom). Based on the numerical results, force–displacement responses, and observed failure patterns, the following conclusions are drawn:

1. Full boundary confinement (four-side support) significantly enhances the out-of-plane resistance, stiffness, and ductility of masonry infills through a two-way arching mechanism. Quantitatively, four-side-supported walls exhibited approximately 73% higher out of plane resistance than three-side-supported walls and 34% higher than two-side-supported walls, demonstrating the substantial effect of complete confinement.
2. Horizontal confinement (top and bottom support) provides better out-of-plane performance than vertical edge confinement alone, highlighting the critical role of horizontal boundaries in resisting lateral inertial forces.
3. Partial confinement (three-side support), particularly with the top edge unrestrained, results in reduced out-of-plane resistance and premature failure under high acceleration levels, indicating that leaving the top edge free can significantly compromise seismic performance.
4. Minimal connection (single-side support) offers negligible resistance to out-of-plane loads and leads to immediate collapse, confirming that this configuration is unsafe under seismic excitations.
5. The effectiveness of masonry infill walls in seismic performance depends not only on material properties but also critically on boundary support conditions. These findings underscore the importance of considering support configurations in both new constructions and retrofitting strategies, as appropriate confinement can substantially improve wall stability, energy dissipation, and overall seismic performance.

Author Contributions

Author 1 Conceptualization, Methodology, Software (Abaqus Modeling), Formal Analysis, Writing – Original Draft; Author 2 conducted the supervision and Methodology, Validation, Writing – Review & Editing. Author 3 developed the Formal Analysis, Validation, Writing – Review & Editing. Authors 3–7 contributed to Writing – Original Draft and Writing – Review & Editing. The manuscript was written through the contribution of all authors. All authors discussed the results, reviewed, and approved the final version of the manuscript.

Acknowledgments

The authors would like to express their sincere gratitude to the Computational Center of the Faculty of Civil Engineering at Shahrood University of Technology for providing access to the necessary systems and computational resources that facilitated the analysis conducted in this study.

Conflict of Interest

The author(s) declared no potential conflicts of interest concerning the research, authorship, and publication of this article.

Funding

The author(s) received no financial support for the research, authorship, and publication of this article.

Data Availability Statements

The datasets generated and/or analyzed during the current study are available from the corresponding author on reasonable request.

Nomenclature

Area of the opening	A_O
Area of the masonry infill	A_P
Shear strength	C
Diagonal length of the opening	d_O
Elastic modulus of mortar and brick units, respectively	E_m , E_u
Compressive strength of brick or masonry unit	f_c
Tensile strength of brick or masonry unit	f_t
Shear modulus of mortar and brick units, respectively	G_m , G_u
Tensile softening energy	G_f^{I}
Shear softening energy	G_f^{II}
Thickness of mortar joint	h_m
Height of opening	h_O
Normal stiffness of joints	k_{nn}
Shear stiffness of joints in two directions	k_{ss}, k_{tt}
Length of opening	l_O
Poisson's ratio	ν
Density of masonry materials	ρ
Thickness of masonry infill	t
Normal and the two shear tractions	t_n , t_s , t_t

References

[1] A. Furtado, H. Rodrigues, A. Arêde, and H. Varum, "Experimental evaluation of out-of-plane capacity of masonry infill walls," *Engineering Structures,* vol. 111, pp. 48-63, 2016.

[2] K. Q. Walsh, D. Y. Dizhur, J. Shafaei, H. Derakhshan, and J. M. Ingham, "In situ out-of-plane testing of unreinforced masonry cavity walls in as-built and improved conditions," in *Structures*, 2015, vol. 3: Elsevier, pp. 187-199.

[3] A. Furtado, H. Rodrigues, A. Arêde, and H. Varum, "Out-of-plane behavior of masonry infilled RC frames based on the experimental tests available: A systematic review," *Construction and Building Materials,* vol. 168, pp. 831-848, 2018.

[4] A. Hashemi and K. M. Mosalam, "Shake-Table Experiments on Masonry Infilled RC Frames," *Journal of Structural Engineering,* 2006.

[5] R. Angel and D. P. Abrams, "Out-of-Plane Strength of Masonry Infill Panels," ed, 1994.

[6] A. A. Tasnimi and M. J. Zamordian, "Effect of Boundary Condition on Infill Panel Behavior," *Asian Journal of Civil Engineering,* 2010.

[7] M. Kumarani and et al., "In-Plane and Out-of-Plane Interaction in Infilled Frames," *Engineering Structures,* 2011.

[8] J. L. Dawe and C. K. Seah, "Out-of-Plane Resistance of Concrete Masonry Infilled Panels," *Canadian Journal of Civil Engineering,* 1989.

[9] P. Negro and G. Verzeletti, "Effect of Infills on the Global Behaviour of R/C Frames," *Earthquake Engineering and Structural Dynamics,* 1996.

[10] D. Daphnis and et al., "Out-of-Plane Response of Masonry Infills," ed, 2002.

[11] M. Ando and et al., "Experimental Study on Out-of-Plane Behavior of Infill Walls," ed, 2006.

[12] Y. Liu and et al., "Finite Element Modelling of Masonry Infilled RC Frames," *Engineering Structures,* 2011.

[13] A. Rabinovich and M. Madah, "Numerical Modelling of Infilled Frame Behavior," *International Journal of Civil Engineering,* 2011.

[14] A. Furtado and et al., "Seismic Behaviour of Masonry Infill Walls," *Bulletin of Earthquake Engineering,* 2015.

[15] Z. Wang, "Dynamic Analysis of RC Frames with Masonry Infill," *Structural Engineering International,* 2017.

[16] H. Y. Noh and et al., "Geometrical Influence on Infill Behavior," *Journal of Earthquake Engineering,* 2019.

[17] M. Di Domenico and et al., "Partial Support Effects in Masonry Infill Walls," *Engineering Structures,* 2021.

[18] S. Messali and et al., "Evaluation of Interaction Effects in Masonry Infill Frames," *Soil Dynamics and Earthquake Engineering,* 2020.

[19] S. Timoshenko and S. Woinowsky-Krieger, "Theory of plates and shells," 1959.

[20] A. W. Hendry, "The lateral strength of unreinforced brickwork," 1973.

[21] A. Hendry and A. Kheir, "The lateral strength of certain brickwork panels," in *Proceedings of the Fourth International Brick Masonry Conference*, 1976, p. 4.

[22] B. A. Haseltine, "Design of laterally loaded wall panels," 1975.

[23] P. Asteris, L. Cavaleri, F. Di Trapani, and A. Tsaris, "Numerical modelling of out-of-plane response of infilled frames: State of the art and future challenges for the equivalent strut macromodels," *Engineering Structures,* vol. 132, pp. 110-122, 2017.

[24] E. McDowell, K. McKee, and E. Sevin, "Arching action theory of masonry walls," *Journal of the Structural Division,* vol. 82, no. 2, pp. 915-1-915-18, 1956.

[25] F. Anić, D. Penava, L. Abrahamczyk, and V. Sarhosis, "A review of experimental and analytical studies on the out-of-plane behaviour of masonry infilled frames," *Bulletin of Earthquake Engineering,* vol. 18, no. 5, pp. 2191-2246, 2020.

[26] A. Mansouri, M. S. Marefat, and M. Khanmohammadi, "Experimental evaluation of seismic performance of low-shear strength masonry infills with openings in reinforced concrete frames with deficient seismic details," *The Structural Design of Tall and Special Buildings,* vol. 23, no. 15, pp. 1190-1210, 2014.

[27] I. ABAQUS, "ABAQUS Theory User Manual," ed: Version, 2011.

[28] J. Shafaei, A. Hosseini, and M. S. Marefat, "Seismic retrofit of external RC beam–column joints by joint enlargement using prestressed steel angles," *Engineering Structures,* vol. 81, pp. 265-288, 2014.

[29] A. Furtado, H. Rodrigues, A. Arêde, and H. Varum, "Experimental characterization of the in-plane and out-of-plane behaviour of infill masonry walls," *Procedia Engineering,* vol. 114, pp. 862-869, 2015.

ORCID iD

Delaram Ostad —

Jalil Shafaei https://orcid.org/0000-0002-7590-4042

Farnoosh Basaligheh —

Mohammad Javad Zarei —

Mohammad Javad Esmaeili —

Milad Faraji —

Amirali Fakor Yekta —

Use this format to cite this article:
Ostad, D., Shafaei, J., Basaligheh, F., Zarei, M. J., Esmaeili, M. J., Faraji, M., Fakor Yekta, A., "Numerical Investigation of the Effect of Boundary Conditions on the Out-of-Plane Seismic Performance of Masonry Infill Walls," *Journal of Structural and Earthquake Engineering*, 1(2), pp. 1–13, 2025.